Novel perturbation method for judging the stability of the equilibrium solution in the presence of passive harmonic cavities

Tianlong He*

National Synchrotron Radiation Laboratory, University of Science and Technology of China, Hefei, Anhui, 230029, People's Republic of China

(Received 15 June 2022; accepted 15 September 2022; published 29 September 2022)

When using the harmonic cavity to stretch the beam in electron storage rings, we expect the beam can be lengthened effectively and also stably. Semianalytical approaches can be used to obtain the equilibrium distribution but generally failed in the prediction of its stability. In this work, a novel perturbation method is proposed to check whether the calculated equilibrium solution can survive from the $l = 1$ mode perturbation. For the case of uniform beam filling, we derive a simple formula that can determine the threshold of $l = 1$ mode instability under specific parameters, which is well verified with tracking simulation for the Hefei Advanced Light Facility storage ring.

DOI: 10.1103/PhysRevAccelBeams.25.094402

I. INTRODUCTION

This study can be regarded as a follow-up to the previous one [1]. In that study, with the high efficiency tracking program-STABLE [2] and a semianalytical calculation approach [3], we are able to use the parameter scanning method to investigate the characteristics of a new beam-loading effect for the Hefei Advanced Light Facility (HALF) storage ring [4], i.e., periodic transient beam-loading (PTBL) effect [1] or called slow moving transient instability [5] or mode 1 instability [6] by other researchers. This PTBL should be avoided, otherwise, it will severely deteriorate the bunch lengthening performance of a harmonic cavity (HC). Besides HALF, the PTBL has also been observed in simulations for SOLEIL-U [5] and Diamond-II [7] and even experimentally at MAX-IV [6]. We believe that the PTBL is also an important common problem for other ultralow emittance storage rings with high average current and employing HC for bunch lengthening.

We find that the semianalytical method originally proposed for the equilibrium solution can also predict the PTBL threshold well, and even the resulting bunch profiles are in good agreement with that obtained by tracking simulation [1]. This inspires us to go deep into the semianalytical method [3] and thus leads us to find a novel perturbation method. Based on this method, we could derive a threshold formula that clearly specifies the condition that the PTBL will occur. We will show that the PTBL is actually derived from the $l = 1$ mode phase perturbation. When satisfying that condition, this $l = 1$ mode perturbation will continue to grow and eventually evolve into PTBL. We call it PTBL to focus on its final behavior while we call it mode 1 instability to focus on its cause. In the following, we will not distinguish between the two statements.

It is worth mentioning that as early as 2018, Venturini used the perturbation-theory mode analysis method to investigate this $l = 1$ mode instability based on the equilibrium distribution and concluded that this instability is driven by the imaginary part of the impedance rather than the real part [8]. The perturbation method proposed here is quite different from that method and can be regarded as a steady-state time-domain perturbation method. That is because we assume the phase perturbation applied to the equilibrium distribution can exist for a long time and then judge whether the perturbation is growing or decaying. For simplicity, this paper only focuses on the case of uniform filling with only the fundamental mode beam-loading effect of the passive HC.

The content of the paper is summarized as follows: In Sec. II, we briefly review the semianalytical method to obtain the equilibrium distribution for the case of uniform beam filling. Sections III A and III B give introductions to, respectively, the main idea of the perturbation method and the exact form of this perturbation. In Sec. III C, we show how to express the steady-state harmonic voltage seen by one bunch. Then in Sec. III D, we derive a formula to obtain the new perturbation phase distribution. In Sec. III E, we define an amplification factor to judge the stability of the equilibrium solution. The dependence of the amplification factor on the HC detuning is discussed in Sec. III F. More details about the derivations can be found in the

*htlong@ustc.edu.cn

Appendixes. In Sec. IV, the threshold formula is well verified through tracking simulation. We make more discussions on the threshold formula in Sec. V. The final conclusion is given in Sec. VI.

II. EQUILIBRIUM SOLUTION

For the case of uniform filling, if there is no instability, the harmonic voltage excited by the beam can be given as

$$V_{hc} = -2FI_0R\cos(\psi_h)\sin(n\varphi + \pi/2 - \psi_h + \varphi_F), \quad (1)$$

where I_0 is the average beam current, n is the harmonic number of HC, R is the HC shunt impedance, and ψ_h is the detuning angle defined in the range of 90°–180°, which can be determined by the below formula

$$\tan(\psi_h) = -\frac{2Q\Delta\omega}{\omega_r}, \quad (2)$$

with Q, $\Delta\omega$, and ω_r being the quality factor, angular detuning frequency, and resonant frequency of HC, respectively. F and φ_F are the amplitude and phase of the bunch form factor, respectively. For a bunch with a given density distribution $\lambda(\tau)$, its bunch form factor can be calculated by

$$\tilde{F} = \int_{-\infty}^{\infty} \lambda(\tau)\exp(-j\omega_r\tau)\,d\tau. \quad (3)$$

If the distribution is symmetric at $\tau = 0$, $\tilde{F}$ is a scalar with $\varphi_F = 0$, otherwise, $\tilde{F}$ is a complex.

For the passive HC, its detuning can be adjusted to make its voltage reach a required ratio relative to that of the main cavity, in order to obtain the required bunch lengthening. Here we denote the required HC voltage amplitude as $\xi V_{\rm rf}$, with ξ, the ratio, and $V_{\rm rf}$, the main voltage amplitude. Then the corresponding detuning is

$$\Delta\omega = \omega_{\rm rf} n\sqrt{\left(\frac{FI_0R/Q}{\xi V_{\rm rf}}\right)^2 - \frac{1}{4Q^2}}. \quad (4)$$

To lengthen the bunch, we should limit $\Delta\omega = \omega_r - n\omega_{\rm rf}$ in the range of $0-\omega_0/2$, with ω_0 the angular revolution frequency and $\omega_{\rm rf}$, the rf fundamental frequency.

The main cavity voltage can be written as $V_{\rm mc} = V_{\rm rf}\sin(\varphi + \varphi_s)$, with φ_s, the synchronous phase. The total cavity voltage of the double rf system can thus be given as

$$V_T = V_{\rm rf}\sin(\varphi + \varphi_s) + \xi V_{\rm rf}\sin(n\varphi + \varphi_h), \quad (5)$$

where $\xi = -2FI_0R\cos(\psi_h)/V_{\rm rf}$ and $\varphi_h = \pi/2 - \psi_h + \varphi_F$. Ignoring the effect of short-range wake, Eq. (5) can be used to calculate the potential $\Phi(\varphi)$ and then the density distribution $\lambda(\varphi)$ ($\varphi = \omega_{\rm rf}\tau$).

$$\Phi(\varphi) = \frac{eV_{\rm rf}}{2\pi h\alpha_c E_0\sigma_\delta^2}\left\{\cos(\varphi_s) - \cos(\varphi + \varphi_s) + \frac{\xi}{n}[\cos(\varphi_h) - \cos(n\varphi + \varphi_h)] - \frac{U_0\varphi}{eV_{\rm rf}}\right\}, \quad (6)$$

$$\lambda(\varphi) = \frac{\exp[\Phi(\varphi)]}{\int_{-\infty}^{\infty}\exp[\Phi(\varphi)]d\varphi}, \quad (7)$$

where e is the elementary charge, h is the harmonic number, α_c is the momentum compaction, E_0 is the design beam energy, and σ_δ is the relative energy spread. The equilibrium distribution can be obtained by iterative calculation with the above equations [9]. It should be noted that this method based on Eq. (1) can only be suitable for the uniform filling case. Hence we call it a simple semianalytical method which is different from the advanced semianalytical methods that can cover the case of the arbitrary filling pattern [10] and arbitrary short-range wake [3,11].

Using this simple semianalytical method, we will find that in order to reach the flat potential (or called optimum lengthening) condition which requires that the first and second derivatives of the total cavity voltage are zero [12], it needs to be put forward requirements only for the value of R instead of R/Q under specific beam current. This case is common when using normal conducting HC. However, for the case of superconducting HC, the flat potential condition is generally impossible due to the very large R. Second best, we can pursue the near-flat potential (or called near-optimum lengthening) condition, that is, to keep the first derivative of the total voltage zero [5].

It should be emphasized that the simple semianalytical method, which defaults that the HC voltage excited by the beam can be expressed as Eq. (1), is incomplete. In fact, the beam may encounter instability, resulting in Eq. (1) that does not hold anymore. It is known that the possible instability is heavily dependent on the value of R/Q but not R. Therefore, after obtaining the equilibrium solution, it is necessary to further analyze whether it can exist stably in order to optimize the design parameters of HC. The conventional approach is to solve the linearized Vlasov equation with perturbation-theory mode analysis [8]. Alternatively, we can also investigate the instability directly by using tracking simulation or a semianalytical approach [1]. Inspired by the semianalytical approach raised in [3], we propose a novel perturbation approach as another complementary approach. It will be shown later that this approach can allow us to derive a simple formula that determines the threshold of $l = 1$ mode instability which can help us efficiently judge whether the parameters of HC are feasible.

III. PERTURBATION METHOD

A. The general philosophy

Suppose we have obtained the equilibrium solution based on the equilibrium assumption, an artificial perturbation phase is then applied to each bunch. This perturbation is small enough and will not cause changes in bunch profiles but will only cause changes in bunch-centroid positions. What we need to do is to solve the new perturbation phase and then compare the two perturbations. If the new one has a larger amplitude, instability will occur, otherwise, it will not.

B. Sinusoidal-perturbation phase distribution

For the case of m bunches uniformly distributed in h buckets (so h/m is an integer), all bunches are identical at equilibrium. We label these bunches as $1, 2, \ldots, m$ to distinguish them. Since they are identical, the initial perturbation phase distribution can be set starting from any one of them, particularly from the bunch labeled as 1. We set that the perturbation phase distribution is sinusoidal and exhibits a coupling mode $l = 1$. We emphasize that it should be done due to the fact that the $l = 1$ mode instability has already been generally verified via numerical solution of linearized Vlasov equation [8], semianalytical calculation, and macroparticle tracking simulation [1]. Certainly, we can also set the perturbation with other coupling modes $l > 1$. This paper focuses on the instability relevant to the $l = 1$ mode. The corresponding perturbation phase distribution can be given in discrete form as

$$\Delta\varphi_i = \epsilon \sin\left[(i-1)\frac{2\pi}{m}\right] (i = 1, 2, \ldots, m), \tag{8}$$

where ϵ represents the perturbation amplitude, which is a very small quantity, e.g., $\epsilon = 10^{-10}$. Note that in Eq. (8), bunch 1 is at phase zero by default.

C. Harmonic voltage at equilibrium

For an electron bunch with charge q and complex form factor $\tilde{F} = F\exp(j\varphi_F)$, the harmonic voltage phasor excited by its first pass through HC is known as $\tilde{F}\frac{q\omega_r R}{Q}$. After its second pass, the voltage phasor becomes $\tilde{F}\frac{q\omega_r R}{Q}(1 + \exp[(j - 1/2Q)\omega_r T_0])$ [3]. By analogy, after its kth pass, the voltage phasor can be written as

$$\tilde{V}_0 = \tilde{F}\frac{q\omega_r R}{Q}\sum_{i=0}^{k}\exp[(j - 1/2Q)\omega_r T_0 i]. \tag{9}$$

When k is large enough, the harmonic voltage tends to a convergent, which can be given by simplifying Eq. (9) as

$$\tilde{V}_0 = \tilde{F}\frac{q\omega_r R}{Q}\frac{1}{1 - \exp[(j - 1/2Q)\omega_r T_0]}, \tag{10}$$

where R/Q is the characteristic parameter of HC, fully determined by the cavity shape, and T_0 is the revolution time. Considering the angular detuning $\Delta\omega = \omega_r - n\omega_{rf}$ and $\omega_{rf} = 2\pi h/T_0$, so $q\omega_r \approx 2\pi n I_0 h/m$ and $\exp[(j - 1/2Q)\omega_r T_0] = \exp(j\Delta\omega T_0)\exp(-\frac{\omega_r T_0}{2Q})$. Substituting both into Eq. (10) (see Appendix A for more details), we can finally get

$$\tilde{V}_0 = \frac{2\pi n F h I_0 R/Q}{m\sqrt{1 + a^2 - 2a\cos(\theta)}}\exp\left[j\left(\frac{\pi - \theta}{2} - \Delta\theta + \varphi_F\right)\right], \tag{11}$$

where $a = \exp(-\frac{\omega_r T_0}{2Q})$, $\theta = \Delta\omega T_0 \in [0, \pi]$ and $\Delta\theta = \arcsin[\frac{1-a}{\sqrt{1+a^2-2a\cos(\theta)}}\cos(\frac{\theta}{2})]$. It should be noted that the value of φ_F depends on how to set the reference phase ($\varphi = 0$). Even if the bunch distribution is completely Gaussian, φ_F will not be zero as long as its axis of symmetry is not at $\varphi = 0$. In order words, we can select a special reference phase so that $\varphi_F = 0$ for arbitrary bunch distribution. Actually, this reference phase is close to that of a bunch centroid. In the following, we take the bunch centroid as the reference, then Eq. (11) can be reduced as (see Appendix B for more details)

$$\tilde{V}_0 = \frac{2\pi n F h I_0 R/Q}{m\sqrt{1 + a^2 - 2a\cos(\theta)}}\exp\left[j\left(\frac{\pi - \theta}{2} - \Delta\theta\right)\right]. \tag{12}$$

Let us now consider the steady-state harmonic voltage phasors contributed by all other bunches, as shown in Fig. 1, these contributions can be treated as that of $\tilde{V}_0$ after rotating counterclockwise for certain angles and having amplitudes attenuated somewhat. For example, the rotation angles of the adjacent bunches before (bunch m) and after

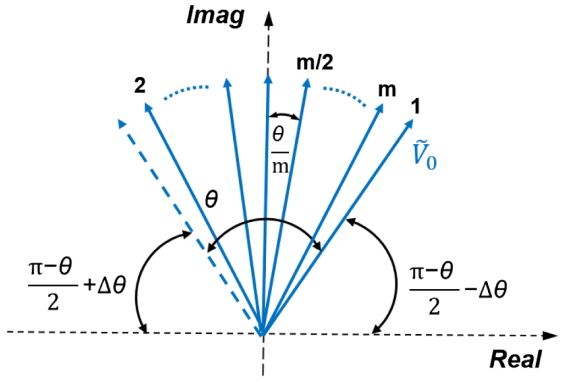

FIG. 1. Schematic of steady-state harmonic voltage phasors contributed by all bunches at the reference phase for bunch 1.

(bunch 2) bunch 1 are $\frac{1}{m}\theta$ and $\frac{m-1}{m}\theta$, respectively, and the corresponding amplitude attenuation coefficients are $\exp(-\frac{\omega_r T_0}{2Q}\frac{1}{m})$ and $\exp(-\frac{\omega_r T_0}{2Q}\frac{m-1}{m})$, respectively. In this way, the contributions of other bunches are not difficult to be drawn from Fig. 1. For the sake of simplifying the following calculations, we reselect the virtual axis shown in Fig. 1 as the reference and rearrange the phasors in counterclockwise order. Then the rotation angles and amplitude attenuation coefficients can be written in the following discrete forms:

$$\theta_k = \frac{\theta}{2} + \Delta\theta - \frac{k-1}{m}\theta, \tag{13}$$

$$d_k = \exp\left(-\frac{\omega_r T_0}{2Q}\frac{k-1}{m}\right), \tag{14}$$

where $k = 1, 2, \ldots, m$. With Eqs. (13) and (14), the total steady-state harmonic voltage seen by one bunch can be written as

$$V_{hc} = |\tilde{V}_0| \sum_{k=1}^{m} d_k \sin(\theta_k). \tag{15}$$

D. Influence of the perturbation phase

When the sinusoidal-perturbation phase distribution is imposed on the bunch centroids and it is assumed that this perturbation exists for a long time, the existence of the perturbation will change the phase of the harmonic voltage phasor and make it rotate at a slight angle. The rotation direction depends on the relative value of the perturbation phases of the two bunches. For the ith bunch, its harmonic voltage considering the influence of the perturbation can be expressed as

$$V_{hc,i} = |\tilde{V}_0| \sum_{k=1}^{m} d_k \sin[\theta_k - n(\Delta\varphi_i - \Delta\varphi_k)], \tag{16}$$

where $\Delta\varphi_k = \epsilon \sin[(i-k)\frac{2\pi}{m}]$, which is given in the order consistent with Eqs. (13) and (14).

Comparing Eqs. (15) and (16), it is easy to obtain the variation of the harmonic voltage caused by the applied perturbation phase, which is

$$\Delta V_{hc,i} = -|\tilde{V}_0| n\epsilon \sum_{k=1}^{m} \epsilon_i^k d_k \cos(\theta_k), \tag{17}$$

where $\epsilon_i^k = \sin[(i-1)\frac{2\pi}{m}] - \sin[(i-k)\frac{2\pi}{m}]$.

Because the bunch centroid is chosen as the reference, the main voltage at the bunch centroid should be expressed as (see Appendix B for more details)

$$V_{mc} = V_{\mathrm{rf}} \sin(\varphi_s - \varphi_F/n), \tag{18}$$

where φ_s and φ_F can be obtained directly from the equilibrium solution.

The change of harmonic voltage will drive the bunch centroid toward a new perturbation phase, denoted by $\Delta\varphi_i'$. As a consequence, the corresponding change of main voltage using the new perturbation phase can be written as

$$\Delta V_{mc,i} = V_{\mathrm{rf}} \cos(\varphi_s - \varphi_F/n)\Delta\varphi_i'. \tag{19}$$

The change of main voltage should be equal to that of harmonic voltage, then the new perturbation phase can be obtained as

$$\begin{aligned}\Delta\varphi_i' &= \frac{\Delta V_{hc,i}}{V_{\mathrm{rf}} \cos(\varphi_s - \varphi_F/n)} \\ &= \frac{|\tilde{V}_0| n\epsilon \sum_{k=1}^{m} \epsilon_i^k d_k \cos(\theta_k)}{V_{\mathrm{rf}} |\cos(\varphi_s - \varphi_F/n)|} \\ &= \frac{2\pi n^2 F h I_0 R/Q\epsilon}{V_{\mathrm{rf}} |\cos(\varphi_s - \varphi_F/n)|} f(\theta, m, i),\end{aligned} \tag{20}$$

where $f(\theta, m, i)$ has the form

$$f(\theta, m, i) = \frac{\sum_{k=1}^{m} \epsilon_i^k d_k \cos(\theta_k)}{m\sqrt{1 + a^2 - 2a\cos(\theta)}}. \tag{21}$$

E. Amplification factor

Given the initial perturbation phase distribution and assuming that it remains for a long time, we can obtain a new perturbation phase distribution using Eqs. (20) and (21). Obviously, if the new perturbation phase distribution has a larger amplitude than the original one, it indicates that the perturbation will continue to grow and eventually lead to an instability. Conversely, it will be suppressed. For the case where m is an integral multiple of 4, it is found that the bunch at the initial perturbation phase of $\pi/2$ (corresponding to $i = m/4 + 1$) or $3\pi/2$ (corresponding to $i = 3m/4 + 1$) has the largest perturbation growth (see Appendix C for more details). Thus, either one of the two bunches can be chosen as the marker to evaluate the $l = 1$ mode instability. According to this, we can introduce an amplification factor for the initial perturbation as

$$\begin{aligned}\eta &= \frac{\max(\Delta\varphi_i')}{\max(\Delta\varphi_i)} \\ &= \frac{\Delta\varphi_{m/4+1}'}{\Delta\varphi_{m/4+1}} \\ &= \frac{2\pi n^2 F h I_0 R/Q}{V_{\mathrm{rf}} |\cos(\varphi_s - \varphi_F/n)|} f(\theta, m),\end{aligned} \tag{22}$$

where the bunch corresponding to $i = m/4 + 1$ is chosen as the marker and thus $f(\theta, m)$ has the form

$$f(\theta, m) = \frac{\sum_{k=1}^{m} \epsilon^{k}_{m/4+1} d_k \cos(\theta_k)}{m\sqrt{1 + a^2 - 2a\cos(\theta)}}, \tag{23}$$

where $\epsilon^{k}_{m/4+1} = \sin(\pi/2) - \sin(\frac{\pi}{2} - k\frac{2\pi}{m})$. It is evident that for the $l = 1$ mode perturbation to be stable, one must have $\eta < 1$.

F. Effect of Q and m on $f(\theta, m)$

As can be seen from Eq. (23), $f(\theta, m)$ is determined by bunch number m, detuning frequency, and Q value of HC. Here we take the HALF storage ring as an example to analyze the dependency of $f(\theta, m)$ on these three parameters. The HALF parameters [4] are listed in Table I. Two different Q values are taken into account: one is 5×10^5 corresponding to superconducting HC and the other is 3×10^4 corresponding to normal conducting HC. Keeping the average current at 350 mA, three different m values are also considered. The results calculated with Eq. (23) are shown in Fig. 2, where the top plot illustrates the values of $f(\theta, 800)$ as a function of the detuning $\Delta f = \Delta\omega/2\pi$, and the bottom plot shows the relative deviations of $f(\theta, 8)$ and $f(\theta, 80)$ to $f(\theta, 800)$, respectively.

From the top plot of Fig. 2, it can be seen that $f(\theta, 800)$ decreases with the detuning, indicating that increasing the detuning is conducive to avoiding the growth of $l = 1$ mode perturbation. In other words, when reducing the detuning to further stretch the bunch length, $f(\theta, 800)$ will be significantly increased especially at lower detuning, thus increasing the possibility of $l = 1$ mode instability. It can also be seen that when the detuning is large, increasing detuning cannot effectively reduce $f(\theta, 800)$ anymore, implying that there exists a possibility that the amplification factor is always larger than 1 no matter how to adjust the detuning. In this case, the $l = 1$ mode is always unstable. This possibility with the specific case will be verified by the tracking simulation later.

TABLE I. HALF parameters with superconducting (SC) or normal conducting (NC) cavity used for the following calculations.

Parameter	Symbol	Value
Circumference	C	480 m
Beam energy	E_0	2.2 GeV
Beam current	I_0	350 mA
Momentum compaction	α_c	9.4×10^{-5}
Energy relative spread	σ_δ	7.44×10^{-4}
Harmonic number	h	800
Main cavity voltage	V_{rf}	1.2 MV
Energy loss with IDs	U_0	400 keV
HC harmonic number	n	3
HC quality factor (SC/NC)	Q	$5 \times 10^5/3 \times 10^4$
HC R/Q	R/Q	41/82 Ω
HC near-optimal detuning	Δf	57/112 kHz

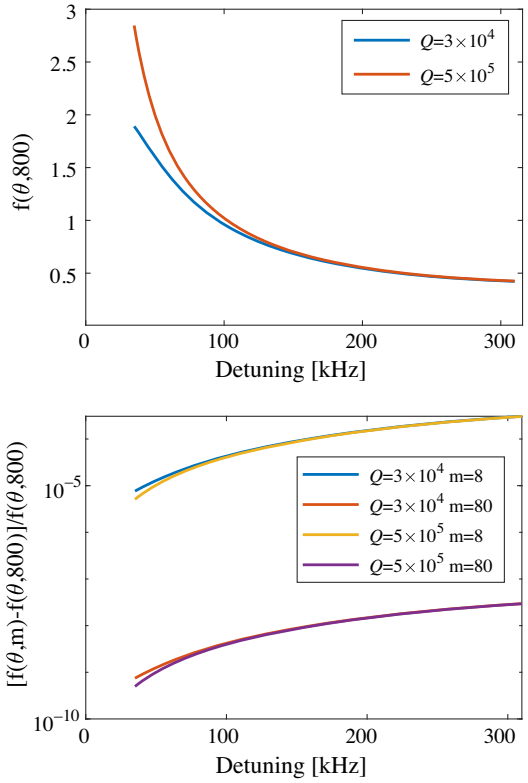

FIG. 2. The value of $f(\theta, 800)$ (top) and the relative deviations of $f(\theta, 8)$ and $f(\theta, 80)$ to $f(\theta, 800)$ (bottom) as functions of detuning.

We note that the effect of Q on $f(\theta, 800)$ is slight for the detuning larger than 150 kHz. While the $f(\theta, 800)$ of normal conducting Q is significantly smaller than that of superconducting Q for the detuning lower than 100 kHz. Nevertheless, this does not mean that the case of normal conducting cavities is more beneficial to decrease the amplification factor because it very likely has the larger total R/Q-values. Here we take the HALF storage ring for example. If the superconducting cavity is adopted, only one cell is required, with R/Q of about 41 Ω and near-optimum detuning of 57 kHz. However, if normal conducting cavities are employed, at least four ALS-U-like cavities [13] can meet the requirements of HALF, leading to the total R/Q of about 82Ω and near-optimum detuning of about 112 kHz. The amplification factor for the two cases of superconducting and normal conducting can be obtained as 0.974 and 0.994, respectively. Therefore, for HALF, the superconducting cavity scheme is more beneficial to avoid $l = 1$ mode instability.

As can be seen from the bottom plot of Fig. 2, the difference between the cases of $m = 8$ and $m = 800$ slightly increases with the detuning and always is less

than 10^{-3}. The difference between $m = 80$ and $m = 800$ is even smaller than 10^{-7} over the entire detuning range. This shows that for the $l = 1$ mode perturbation, the resulting amplification factors of the three cases are very close to each other. It enlightens us that when we try to perform tracking simulations to study this instability, we can use fewer bunches without affecting the results.

IV. VERIFICATION ON EQ. (22)

A. Threshold of $l = 1$ mode perturbation growth

In order to verify the accuracy of Eq. (22), we intend to compare the difference between the two threshold detunings obtained by both Eq. (22) and tracking simulation with the STABLE code. Using Eq. (22), it is easy to obtain the threshold detuning of HC, which corresponds to $\eta = 1$. In tracking simulation, 80 equally spaced and equally charged bunches are tracked for 500,000 turns and each bunch is represented by 20,000 macroparticles. According to the above analysis, using 80 instead of 800 bunches will not affect the results. We can scan the detuning near the threshold detuning obtained by Eq. (22) to determine the tracking threshold detuning, below which corresponds to the appearance of PTBL. We consider two Q values. For the lower Q, other forms of coupled bunch instability may occur when at large detuning, e.g., in general an $l = 1$ mode coupled bunch instability combined with both dipole and quadrupole Robinson instabilities [14] or an instability with more complex behavior. In order to fully damp them, the damping time in the tracking simulation is set to 0.1 ms. The resulting threshold detunings are shown in Fig. 3.

Let us first look at the results of the larger Q (superconducting case). When higher than 60 Ω of R/Q, the resulting threshold detunings given by both methods are in very good agreement, generally with a difference of less than 1 kHz. When lower than 60 Ω, the difference can reach about 3–4 kHz. In that case, we can obtain more

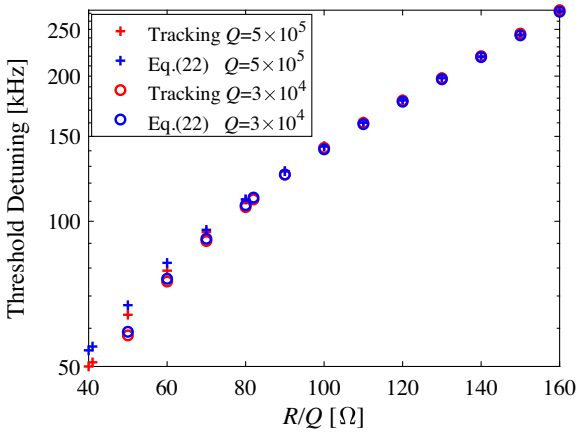

FIG. 3. Threshold detuning obtained by tracking simulation (in red) and using Eq. (22) (in blue).

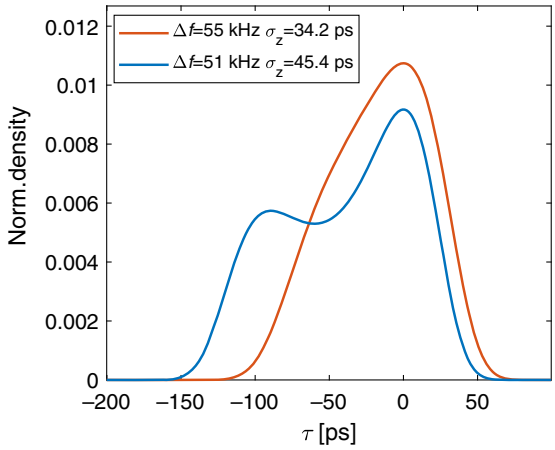

FIG. 4. Bunch density profiles for the case of $R/Q = 41$ Ω and $Q = 5 \times 10^5$.

bunch lengthening by tracking, with the corresponding bunch profile nearly having double bumps (overstretching) and a large bunch form factor phase, e.g., as shown in the bunch profiles of Fig. 4 for the cases of the threshold detuning obtained by Eq. (22) ($\Delta f = 55$ kHz) and tracking simulation ($\Delta f = 51$ kHz). The overstretching regime may cause our treatment method to be no longer accurate enough.

For the lower Q (normal conducting case), the two methods give threshold detunings in good agreement, with a difference of less than 1 kHz. It should be noted that, even above the threshold detuning of $l = 1$ mode, the instability of other modes possibly become a critical problem due to the large R/Q, resulting in a complex instability. To obtain the true threshold detuning of $l = 1$ mode perturbation growth, it is necessary to eliminate the interference of other modes by setting the damping time to 0.1 ms. We emphasize that under such a low damping time setting, we still get the threshold detuning of $l = 1$ mode perturbation growth, which implies that this instability is hardly suppressed by the existing feedback.

We note that for the cases of R/Q higher than 90 Ω, the resulting threshold detunings of both Q-values nearly coincide with each other. It means that in these cases, the $l = 1$ mode instability is very weakly dependent on the Q-value. This conclusion can also be derived straightforward from Eq. (22) and the $f(\theta, 800)$ shown in the top plot of Fig. 2 since both curves are close to each other at detuning larger than 120 kHz.

B. The case of unavoidable $l = 1$ mode perturbation growth

We mentioned earlier that there exists a possibility that $\eta > 1$ always no matter how to adjust the detuning. In that case, the $l = 1$ mode perturbation will finally grow into an instability. For example, in the case of $R/Q = 170$ Ω for

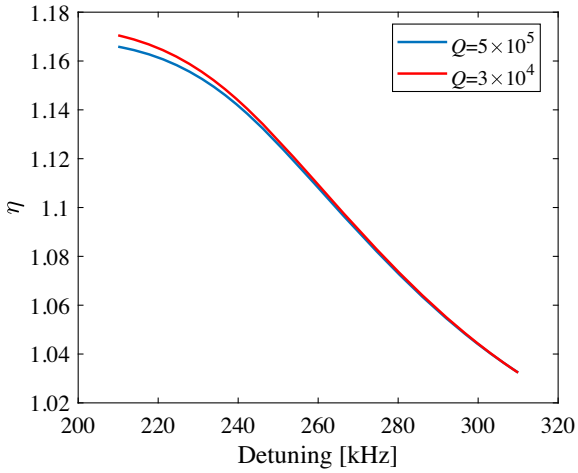

FIG. 5. Amplification factor as a function of detuning for the case of $R/Q = 175\ \Omega$.

the HALF storage ring, the amplification factors obtained with Eq. (22) for both $Q = 5 \times 10^5$ and $Q = 3 \times 10^4$, as shown in Fig. 5, are always larger than 1, predicting an inevitable instability. This prediction has been verified correctly by tracking simulations with the parameters listed in Table I.

V. DISCUSSION ON EQ. (22)

Equation (22) defines clearly the dependence of the amplification factor on relevant parameters. We point out that a PTBL effect in the presence of passive superconducting HC is described in [1], which is exactly developed from the $l = 1$ mode perturbation. Some conclusions relevant to PTBL are drawn by parameter scanning in [1]: (i) The PTBL threshold relies on the product of HC R/Q and average current I_0; (ii) the PTBL threshold increases with the main voltage amplitude and the detuning of HC; and (iii) the PTBL threshold does not depend on the momentum compaction and relative energy spread separately but rather only through their influence on the bunch distribution. Now, these conclusions can be clearly derived from Eq. (22). Besides, it can be found that the $l = 1$ mode threshold depends on the square of the harmonic number of HC. Obviously, the lower harmonic number is more beneficial to avoid PTBL.

Equation (22) provides us with a criterion to determine the possibility of $l = 1$ mode instability under specific parameters. When selecting HC parameters, try to avoid $\eta > 1$, otherwise it is difficult to achieve the required bunch lengthening. Sometimes, if overstretching is necessary, we should assure $\eta < 1$ as far as possible under near-optimal (or optimum) lengthening condition, so as to leave a certain margin for lower detuning.

For the case of overstretching scenario, we find, through tracking simulations, that $\eta > 1$ is not a sufficient clear indication for the $l = 1$ mode instability. More precisely, the threshold detuning obtained by Eq. (22) is generally higher by 3–4 kHz than that by tracking. For the case without overstretching, if we get $\eta < 1$ with Eq. (22), it generally indicates that the $l = 1$ mode perturbation can be fully suppressed.

It should be noted that Venturini reported a critical R/Q formula for the $l = 1$ coupled bunch instability [15], which was found by solving a system of linear algebraic equations and is expected to be accurate for parameters in the neighborhood of the ALS-U HC. This critical R/Q is a very weak function of Q and approximately scales with $\frac{\sigma_\delta}{n^2 I_0}\sqrt{\frac{E_0 \alpha_c V_{\rm rf}}{Fh}}$. Using Eq. (22), we can also obtain a critical R/Q formula, namely

$$(R/Q)_{\rm crit} = \frac{V_{\rm rf}|\cos(\varphi_s - \varphi_F/n)|}{2\pi n^2 F h I_0 f(\theta, m)}. \tag{24}$$

Obviously, the two scaling laws exhibit the same quantitative dependence of the critical R/Q on parameters n and I_0 but a different quantitative dependence on parameters $V_{\rm rf}$, F, and h. In addition, Venturini's formula explicitly includes $\sigma_\delta\sqrt{E_0\alpha_c}$, while our formula implies that this critical R/Q is not directly related to parameters σ_δ, α_c, and E_0, unless they affect the bunch form factor F.

VI. CONCLUSION

By applying a sinusoidal-perturbation phase distribution of $l = 1$ mode to the equilibrium, we derive a threshold formula, i.e., Eq. (22), which can be used to determine whether the $l = 1$ mode perturbation will increase or be suppressed under specific parameters. This formula clearly shows the dependence of the threshold condition of $l = 1$ mode perturbation on relevant parameters, so it can help us select the appropriate parameters to obtain the desired bunch lengthening. Additionally, it predicts an inevitable PTBL for the case of too large R/Q of HC, which has been well verified with tracking simulation. In view of the good verification of the threshold formula, it indicates that PTBL is exactly originated from the $l = 1$ mode perturbation. Under specific parameters, this perturbation will inevitably grow and eventually evolve into PTBL.

ACKNOWLEDGMENTS

This work was supported by National Natural Science Foundation of China (12105284) and the Fundamental Research Funds for the Central Universities (WK2310000090).

APPENDIX A: SIMPLIFY EQ. (10) TO EQ. (11)

Figure 6 shows how to get Eq. (11) from Eq. (10), where $a = \exp(-\frac{\omega_r T_0}{2Q})$ and $\theta = \Delta\omega T_0$. The green arrow represents $1 - \exp[(j - 1/2Q)\omega_r T_0]$. Its amplitude can be obtained using the Law of Cosines of triangle, i.e., $\sqrt{1 + a^2 - 2a\cos(\theta)}$, and its phase with respect to the real axis is $-(\frac{\pi-\theta}{2} - \Delta\theta)$. According to the Law of Sines, we have

$$\frac{\sin(\Delta\theta)}{1-a} = \frac{\sin\left(\frac{\pi-\theta}{2}\right)}{\sqrt{1+a^2-2a\cos(\theta)}}, \tag{A1}$$

so

$$\Delta\theta = \arcsin\left[\frac{1-a}{\sqrt{1+a^2-2a\cos(\theta)}}\cos\left(\frac{\theta}{2}\right)\right], \tag{A2}$$

then we have

$$1 - \exp\left[\left(j - \frac{1}{2Q}\right)\omega_r T_0\right] = \frac{\sqrt{1+a^2-2a\cos(\theta)}}{\exp[j(\frac{\pi-\theta}{2} - \Delta\theta)]}, \tag{A3}$$

so

$$\frac{1}{1 - \exp[(j - \frac{1}{2Q})\omega_r T_0]} = \frac{\exp[j(\frac{\pi-\theta}{2} - \Delta\theta)]}{\sqrt{1+a^2-2a\cos(\theta)}}. \tag{A4}$$

Considering $q\omega_r \approx 2\pi n I_0 h/m$ and $\tilde{F} = F\exp(j\varphi_F)$, we finally have

$$\tilde{V}_0 = \frac{2\pi n F h I_0 R/Q}{m\sqrt{1+a^2-2a\cos(\theta)}}\exp\left[j\left(\frac{\pi-\theta}{2} - \Delta\theta + \varphi_F\right)\right], \tag{A5}$$

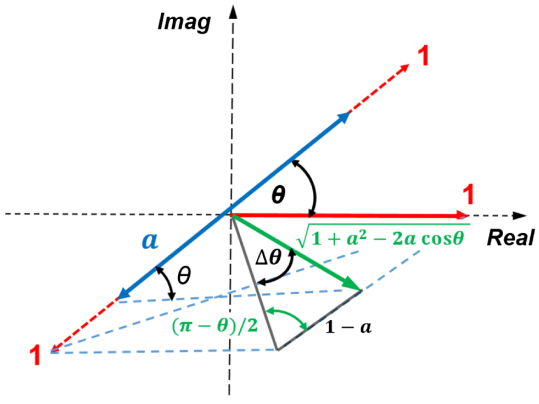

FIG. 6. Schematic diagram of simplifying Eq. (10) to Eq. (11).

If $Q \gg 1$ (for superconducting case), then $a \approx 1$, $\Delta\theta \approx 0$ and the formula (A5) can be reduced to

$$\tilde{V}_0 = \frac{\pi n F h I_0 R/Q}{m\sin\left(\frac{\theta}{2}\right)}\exp\left[j\left(\frac{\pi-\theta}{2} + \varphi_F\right)\right], \tag{A6}$$

APPENDIX B: TAKE THE BUNCH CENTROID AS THE REFERENCE

For the equilibrium distribution obtained by the semi-analytical approach, the bunch centroid generally deviates from $\tau = 0$, e.g., the resulting distribution shown in Fig. 7. This deviation causes the nonzero phase of the bunch form factor, which can affect the beam-loading voltage and should not be neglected. However, if we take the bunch centroid instead of the synchronous phase as the reference (shifting the time zero to the centroid), the corresponding form factor phase is so small that the term φ_F can be dropped in Eq. (12).

Accordingly, considering the influence of the centroid deviation from the synchronous phase, the main voltage seen at bunch centroid should be expressed as

$$V_{mc} = V_{\mathrm{rf}}\sin(\varphi_s + \varphi_{\langle\tau\rangle}). \tag{B1}$$

It is easy to know $\varphi_{\langle\tau\rangle} \approx -\varphi_F/n$. Substituting it into the above formula, it yields

$$V_{mc} = V_{\mathrm{rf}}\sin(\varphi_s - \varphi_F/n). \tag{B2}$$

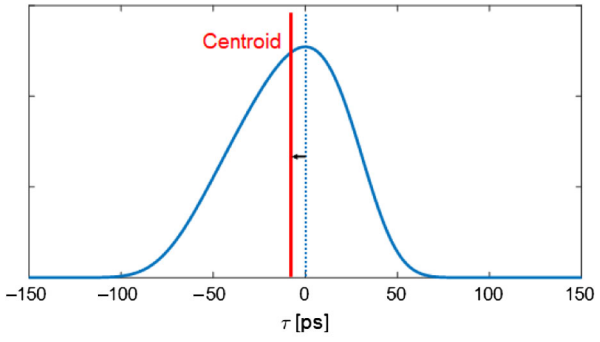

$\varphi_F = 0.08414, \varphi_{<\tau>} = -0.02834$

FIG. 7. Schematic of an asymmetric bunch distribution with nonzero bunch form factor phase. The resulting distribution is obtained with the HC parameters of $R/Q = 90\ \Omega$, $Q = 5 \times 10^5$, and $\Delta f = 125$ kHz. The corresponding form factor phase is 0.08414 and the deviation phase of bunch centroid is $\omega_{\mathrm{rf}}\langle\tau\rangle = -0.02834$, which is negative since the centroid phase is ahead of the synchronous phase. The form factor phase for the reference of bunch centroid is $\varphi_F + n\varphi_{\langle\tau\rangle} = -8.8 \times 10^{-4} \approx 0$.

APPENDIX C: AMPLIFICATION FACTOR DETERMINED WITH THE BUNCH AT PERTURBATION PHASE OF $\pi/2$ OR $3\pi/2$

When imposing the perturbation phase to the equilibrium, the influence of the phase difference among bunches on the harmonic voltage phasor must be considered. Specifically, it will slightly affect the phase of the voltage phasor shown in Fig. 1. For the bunch at perturbation phase of $\pi/2$ or $3\pi/2$, the rotation directions of the voltage phasors caused by the perturbation are the same. Consequently, it has the largest harmonic voltage change, which leads to the largest perturbation phase growth. Let us take an example with four bunches to briefly explain that. Their perturbation phases are shown in Fig. 8, and the influence of the perturbation on their voltage phasors is illustrated in Fig. 9. Obviously, for the first and third bunches, the perturbation makes the voltage phasors contributed by the second and fourth bunches rotate in the opposite direction, causing their effects to partially or even completely cancel each other out. Whereas for the second or fourth bunch, the perturbation rotates the voltage phasors contributed by the other three bunches in the same direction, thus making their effects superimposed on each other. Based on the above analysis, it can be seen that the second ($\pi/2$) and fourth bunches ($3\pi/2$) have the largest harmonic voltage change and thus have the largest perturbation phase growth.

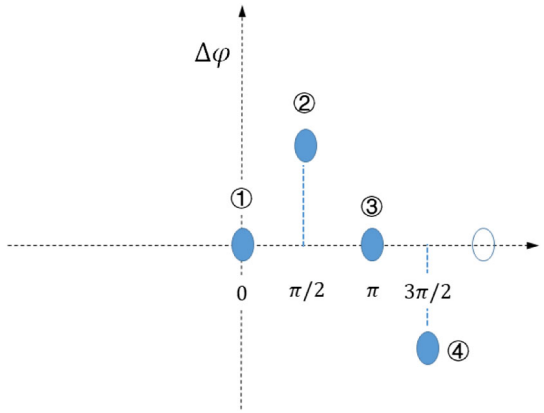

FIG. 8. Schematic of the perturbation phase for the four bunches.

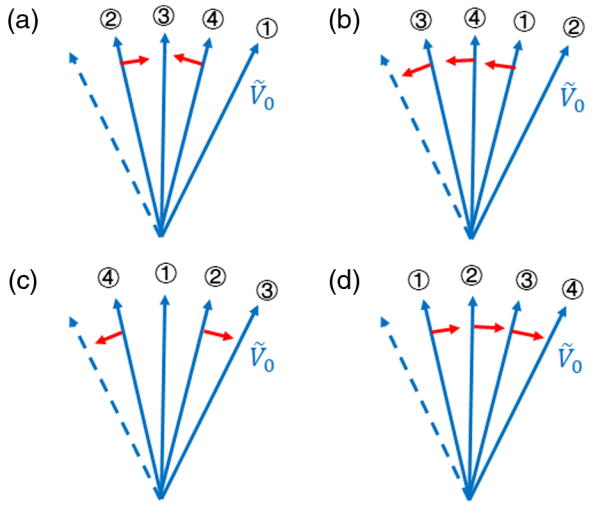

FIG. 9. Schematic of the influence of the perturbation on the voltage phasors. (a) For the first bunch, (b) for the second bunch, (c) for the third bunch, and (d) for the fourth bunch. The red arrow shows the rotation direction of the voltage phasor caused by the perturbation.

[1] T. He, W. Li, Z. Bai, and L. Wang, Periodic transient beam loading effect with passive harmonic cavities in electron storage rings, Phys. Rev. Accel. Beams **25**, 024401 (2022).

[2] T. He and Z. Bai, Graphics-processing-unit-accelerated simulation for longitudinal beam dynamics of arbitrary bunch trains in electron storage rings, Phys. Rev. Accel. Beams **24**, 104401 (2021).

[3] T. He, W. Li, Z. Bai, and L. Wang, Longitudinal equilibrium density distribution of arbitrary filled bunches in presence of a passive harmonic cavity and the short range wakefield, Phys. Rev. Accel. Beams **24**, 044401 (2021).

[4] Z. H. Bai, G. W. Liu, T. L. He, T. Zhang, W. W. Li, P. H. Yang, Z. L. Ren, S. C. Zhang, W. M. Li, G. Y. Feng, and L. Wang, A modified hybrid 6BA lattice for the HALF storage ring, in *Proceedings of 12th International Particle Accelerator Conference, Campinas, SP, Brazil* (JACoW, Geneva, Switzerland, 2021), pp. 407–409, MOPAB112.

[5] A. Gamelin, Harmonic cavity studies for the SOLEIL Upgrade, in *Proceedings of I. FAST Workshop 2022 Beam Diagnostics and Dynamics in Ultra-low Emittance Rings* (2022), https://indico.scc.kit.edu/event/2592/sessions/2579/attachments/5006/7591/Slides_3-1_Gamelin.pdf.

[6] F. Cullinan, Å. Andersson, J. Breunlin, M. Brosi, and P. F. Tavares, Longitudinal beam dynamics in ultra-low emittance rings, in *Proceedings of I. FAST Workshop 2022, Karlsruhe, Germany* (2022), https://indico.scc.kit.edu/event/2592/sessions/2576/attachments/5004/7619/IFASTatKIT2022_Cullinan.pdf.

[7] T. Olsson, Collective effects in the Diamond-II Storage Ring, in *Proceedings of 3rd Workshop on Low Emittance Lattice Design* (2022), https://indico.cells.es/event/1072/contributions/1804/attachments/1300/2424/Diamond-II%20Collective%20Effects%20-%20LEL%202022.pdf.

[8] M. Venturini, Passive higher-harmonic rf cavities with general settings and multibunch instabilities in electron storage rings, Phys. Rev. Accel. Beams **21**, 114404 (2018).

[9] P. F. Tavares, Å. Andersson, A. Hansson, and J. Breunlin, Equilibrium bunch density distribution with passive harmonic cavities in a storage ring, Phys. Rev. ST Accel. Beams **17**, 064401 (2014).

[10] T. Olsson, F. J. Cullinan, and Å. Andersson, Self-consistent calculation of transient beam loading in electron storage

rings with passive harmonic cavity, Phys. Rev. Accel. Beams **21**, 120701 (2018).

[11] R. Warnock, Equilibrium of an arbitrary bunch train with cavity resonators and short range wake: Enhanced iterative solution with Anderson acceleration, Phys. Rev. Accel. Beams **24**, 104402 (2021).

[12] J. M. Byrd and M. Georgsson, Lifetime increase using passive harmonic cavities in synchrotron light sources, Phys. Rev. ST Accel. Beams **4**, 030701 (2001).

[13] T. Luo, K. Baptiste, S. De Santis, D. Li, J. Staples, M. Venturini, and H. Feng, Design progress of ALS-U 3rd-harmonic cavity, in *Proceedings of the IPAC2021, Campinas, SP, Brazil, 2021* (JACoW, Campinas, SP, Brazil, 2021), pp. 1481–1483, TUPAB053.

[14] R. A. Bosch, K. J. Kleman, and J. J. Bisognano, Robinson instabilities with a higher-harmonic cavity, Phys. Rev. ST Accel. Beams **4**, 074401 (2001).

[15] M. Venturini, Semi-analytical studies of HHC instabilities in the ALS-U, in *Proceedings of LER8 Workshop 2020, Frascati, Italy* (2020), https://agenda.infn.it/event/20813/contributions/110227/attachments/76559/98462/Venturini_LER8_Oct2020.pdf.